Increased Antigen Cross-Presentation but Impaired Cross-Priming after Activation of Peroxisome Proliferator-Activated Receptor γ Is Mediated by Up-Regulation of B7H1[1]

Luisa Klotz,[2,3§] Stephanie Hucke,[2*] Dominik Thimm,[*] Sabine Classen,[†] Andrea Gaarz,[†] Joachim Schultze,[†] Frank Edenhofer,[‡] Christian Kurts,[*] Thomas Klockgether,[§] Andreas Limmer,[*] Percy Knolle,[*] and Sven Burgdorf[3*]

Dendritic cells are able to take up exogenous Ags and present Ag-derived peptides on MHC class I molecules, a process termed cross-presentation. The mannose receptor (MR), an endocytic receptor expressed on a variety of APCs, has been demonstrated to target soluble Ags exclusively toward cross-presentation. In this study, we investigated the role of the murine nuclear receptor peroxisome proliferator-activated receptor γ (PPARγ), a ligand-activated transcription factor with immunomodulatory properties, in MR-mediated endocytosis and cross-presentation of the model Ag OVA. We could demonstrate both in vitro and in vivo that activation of PPARγ resulted in increased MR expression, which in consequence led to enhanced MR-mediated endocytosis and elevated cross-presentation of soluble OVA. Concomitantly, activation of PPARγ in dendritic cells induced up-regulation of the coinhibitory molecule B7H1, which, despite enhanced cross-presentation, caused an impaired activation of naive OVA-specific CD8$^+$ T cells and the induction of T cell tolerance. These data provide a mechanistic basis for the immunomodulatory action of PPARγ which might open new possibilities in the development of therapeutic approaches aimed at the control of excessive immune responses, e.g., in T cell-mediated autoimmunity. *The Journal of Immunology,* **2009, 183: 129–136.**

Dendritic cells (DCs)[4] are professional APCs which play an important role in the induction of adaptive immune responses (1). DCs internalize extracellular Ags, process them in specialized intracellular compartments, and present Ag-derived peptides in the context of MHC molecules to T cells. In classical Ag presentation, extracellular Ags are degraded in lysosomes by lysosomal proteases and loaded on MHC class II (MHC II) molecules (1, 2). Recognition of these complexes by Ag-specific CD4$^+$ Th cells is essential for full activation of macrophages, B cells, and CD8$^+$ T cells in vivo. In addition, DCs are capable of presenting extracellular Ags on MHC class I (MHC I) molecules, a process termed cross-presentation (3, 4) that enables DCs to activate Ag-specific cytotoxic CD8$^+$ T cells. Cross-presentation has been shown to be essential for a variety of processes, including the induction of immune responses against viruses that do not infect DCs or against nonhematopoietic tumors (4–7). Recently, our group could demonstrate that the mechanism of Ag uptake by DCs determines whether soluble extracellular Ag is presented on MHC I or on MHC II molecules (8, 9). After pinocytosis or scavenger receptor-mediated endocytosis, the model Ag OVA was targeted rapidly toward lysosomal compartments where it was processed and presented exclusively on MHC II molecules. However, when OVA was taken up via the mannose receptor (MR), it was processed exclusively for cross-presentation (8–10). The MR targeted OVA into a distinct early endosomal compartment, which did not mature further into lysosomes but in which Ag-derived peptides were loaded on MHC I molecules (11). Because cross-presentation was completely abolished in MR-deficient DCs (8), expression of the MR is essential for cross-presentation of OVA-derived peptides on MHC I molecules.

Ag recognition in the context of MHC molecules, commonly referred to as signal 1, is an important prerequisite for T cell activation. However, additional signals like the expression of costimulatory molecules (signal 2) and the secretion of proinflammatory cytokines (signal 3) are required for the induction of a potent adaptive immune response. These signals are provided by DCs that have undergone a maturation process, e.g., upon recognition of microbial substances (12). In the absence of costimulatory molecules or proinflammatory cytokines, naive T cells cannot be activated properly but instead become tolerant. Additionally, T cell tolerance cannot only be induced indirectly, i.e., by lack of costimulatory signals, but also directly by APC-mediated signaling via coinhibitory molecules such as B7H1 or B7DC (also referred

*Institutes of Molecular Medicine and Experimental Immunology, University Hospital Bonn, Bonn, Germany; and †Laboratory for Genomics and Immunoregulation, Institute for Life and Medical Sciences, ‡Institute of Reconstructive Neurobiology, Life and Brain Center, and §Department of Neurology, University of Bonn, Bonn, Germany

Received for publication December 18, 2008. Accepted for publication April 27, 2009.

The costs of publication of this article were defrayed in part by the payment of page charges. This article must therefore be hereby marked *advertisement* in accordance with 18 U.S.C. Section 1734 solely to indicate this fact.

[1] L.K. was supported by Clinical Research Group Grant KFO177 and S.B. and C.K. by Collaborative Research Center Grant SFB645. Both grants were funded by the German Research Foundation.

[2] L.K. and S.H. contributed equally to this work.

[3] Address correspondence and reprint requests to Dr. Luisa Klotz and Dr. Sven Burgdorf, Institutes of Molecular Medicine and Experimental Immunology, University Hospital Bonn, Sigmund-Freud-Strasse 25, 53105 Bonn, Germany. E-mail addresses: luisa.klotz@ukb.uni-bonn.de and Sven.Burgdorf@ukb.uni-bonn.de

[4] Abbreviations used in this paper: DC, dendritic cell; MR, mannose receptor; PPARγ, peroxisome proliferator-activated receptor γ; Pio, pioglitazone; BM-DC, bone marrow-derived DC; MHC I/II, MHC class I/II; HTNCre, His-TAT-NLS-Cre; CPRG, chlorophenol red-β-D-galactopyranoside.

to as PDL1 and PDL2). The interaction of these molecules with PD1 expressed on T cells results in T cell inactivation (13). Hence, DCs influence the outcome of a T cell response not only by presentation of the respective Ag, but also by signaling via costimulatory and coinhibitory molecules and by secretion of proinflammatory cytokines.

A transcription factor that is involved in cell-intrinsic control of DC immunogenicity is the nuclear receptor peroxisome proliferator-activated receptor γ (PPARγ). Upon ligand binding, PPARγ heterodimerizes with the retinoid X receptor and influences gene transcription by binding to PPAR response elements in the promoter region of target genes (14). Additionally, PPARγ can negatively interfere with proinflammatory transcription factors like NF-κB to inhibit transcription of proinflammatory cytokines (15–17). PPARγ agonists include endogenous ligands such as polyunsaturated fatty acids and prostanoids as well as synthetic ligands such as pioglitazone (Pio) (18–20). Due to their immunomodulatory effects, PPARγ agonists have been postulated to be promising agents for therapeutic strategies against autoimmune diseases such as multiple sclerosis and rheumatoid arthritis (21).

Previously, we and others have shown that activation of PPARγ suppresses DC maturation (22, 23). Sustained activation of PPARγ in DCs prevented LPS-induced up-regulation of costimulatory molecules and production of proinflammatory cytokines. In consequence, decreased signaling via signals 2 and 3 resulted in severely impaired priming of $CD4^+$ T cells by PPARγ-activated DCs both in vitro and in vivo (23).

In the present study, we investigated the effect of PPARγ activation on cross-presentation and subsequent activation of cytotoxic $CD8^+$ T cells. We demonstrated both in vitro and in vivo that activation of PPARγ leads to increased uptake and cross-presentation of OVA but concomitantly impaired activation of $CD8^+$ T cells due to increased signaling via the coinhibitory molecule B7H1.

Materials and Methods

Mice

C57BL/6 mice and $PPAR\gamma^{fl/fl}$ mice were purchased from Charles River Laboratories. $MR^{-/-}$ mice on a C57BL/6 background were provided by Dr. M. C. Nussenzweig (Rockefeller University, New York, NY), OT-I Rag-$1^{-/-}$ mice by Dr. W. R. Heath (University of Melbourne, Melbourne, Australia), and $B7H1^{-/-}$ mice from Dr. L. Chen (Johns Hopkins University School of Medicine, Baltimore, MD). For all experiments, mice between 8 and 16 wk of age were bred under specific pathogen-free conditions and used in accordance with local animal experimentation guidelines.

Abs and reagents

Fluorochrome-labeled Abs against CD11c, B7H1, CD40, CD80 CD86, ICOSL, PD1, and CD8α were obtained from eBioscience and anti-MR and anti-B7DC from AbD Serotec. The PD1-specific blocking Ab (clone J43) was obtained from eBioscience. All reagents, if not specified otherwise, were purchased from Sigma-Aldrich.

Generation of bone marrow-derived DCs (BM-DCs)

BM-DCs were generated as described previously (10, 24). Pio (Axxora) was added at a concentration of 10 μM during the whole differentiation procedure as previously described (23).

Conditional PPARγ knockout in BM-DCs

Conditional knockout of PPARγ in BM-DCs was achieved by Cre-mediated site-specific recombination of loxP sites integrated into the PPARγ locus of $PPAR\gamma^{fl/fl}$ mice as described previously (23). Briefly, bone marrow precursor cells derived from $PPAR\gamma^{fl/fl}$ or wild-type mice were isolated and incubated with 3 μM of a membrane-permeable His-TAT-NLS-Cre (HTNCre) recombinase for 6 h, washed extensively, and cultured in the absence of Cre. At day 3, the procedure was repeated and cells were cultivated for another 4 days. During the differentiation procedure, 10 μM Pio was added to the appropriate groups.

Flow cytometry

Flow cytometry, including intracellular staining of the MR, was performed as described previously (8) using a FACSCanto flow cytometer (BD Biosciences). Results were analyzed using FlowJo software (Tree Star).

RNA preparation and microarray hybridization

MR^+ resp MR^- BM-DC ($n = 3$) were purified by FACS and lysed in TRIzol reagent (Invitrogen Life Technologies). RNA isolation and quantification were performed as described previously (25). cRNA (1.5 μg) was hybridized to BeadChip Arrays (MouseWG-6 v2 Expression BeadChip; Illumina) and scanned on Illumina BeadStation 500 X. Raw data collection for Illumina BeadChip Arrays was performed using Illumina BeadStudio software. Further statistical and bioinformatic analyses were performed using R language (http://www.r-project.org) and packages from the Bioconductor project. For normalization of the data, we used quantile normalizations implemented in R. Microarray data are available at the Gene Expression Omnibus database (www.ncbi.nlm.nih.gov/geo; accession no. GSE15616).

Uptake of soluble OVA

BM-DCs were incubated with 3 μg/ml Alexa Fluor 647-labeled OVA for 15 min at 37°C. Cells were harvested, washed, stained with an Ab against CD11c, and analyzed by flow cytometry.

Cross-presentation by BM-DCs monitored by the 25-D1.16 Ab

BM-DCs were incubated for 18 h with 10 mg/ml purified OVA. Afterward, nonspecific binding sites were blocked by PBS containing 50 mg/ml milk powder, 1% mouse serum, and 1% rat serum for 1 h. Subsequently, cells were washed and surface staining was performed using the biotinylated 25D1.16 Ab (provided by R. Germain and J. Yewdell, Bethesda, MD). After extensive washing, cells were incubated with Alexa Fluor 647-conjugated streptavidin for 15 min. Finally, cells were incubated with 1.2 μg/ml Hoechst 33342 to stain for living cells. Cells were examined using an IX81 microscope (Olympus) and analyzed by Scan^R Software (Olympus).

Coculture assays of DCs with B3Z or OT-I T cells

For in vitro experiments, BM-DCs were incubated with 0.5 mg/ml OVA for 2 h and subsequently cocultured with B3Z or OT-I T cells. To determine B3Z activation, the medium was removed after 24 h of coculture and cells were incubated with 0.1 mM chlorophenol red-β-D-galactopyranoside (CPRG). After another 24 h, B3Z activation was analyzed by spectrophotometry (26). OT-I T cell activation was determined by measuring the IFN-γ concentration in the supernatant 48 h after coculture initiation by ELISA. For restimulation, viable $CD8^+$ T cells were harvested at day 5 by density gradient centrifugation and cultured for another 24 h in the presence of 10 μg/ml anti-CD3 as described before (23). Cytokine concentrations in the supernatants were analyzed by ELISA. To analyze proliferation, OT-I T cells were labeled for 10 min with 2.5 μM CFSE and cocultured with BM-DCs for 3 days; proliferation was assessed by flow cytometric analysis of the CFSE dilution.

For experiments using splenic DCs, mice were administered 30 mg/kg body weight Pio (Actos; Takeda Pharmaceuticals) in 0.5% carboxymethylcellulose or the vehicle only by daily oral gavage for 7 days. Forty-five minutes before analysis of MR expression and OVA uptake by splenic DCs, mice were injected with Alexa Fluor 647-labeled OVA (5 μg/g body weight). For coculture assays ex vivo with B3Z cells, mice were injected with 100 μg/g body weight OVA. Forty-five minutes after injection, splenic DCs were isolated using an AutoMACS System (Miltenyi Biotec), cocultured with B3Z cells, and analyzed as described above. For OT-I T cell activation assays, splenic DCs were incubated with 0.5 mg/ml OVA for 2 h before coculture with OT-I T cells as described above. If not indicated differently, cross-priming assays were performed using a DC:T cell ratio of 1:2.

Cytotoxicity assays

In vivo cytotoxicity assays were performed as described previously (27). Briefly, Pio-treated or vehicle-treated wild-type mice were immunized with 10^6 Pio-treated or untreated OVA-loaded BM-DCs s.c. Five days later, target cells were prepared to assess in vivo cytotoxic activity. As target cells, splenocytes were either pulsed with SIINFEKL peptide (1 μg/ml, 15 min at 37°C) and labeled with a high concentration of CFSE (1 μM, 15 min at 37°C; $CFSE^{high}$ cells) or were mock treated and labeled with a low concentration of CFSE (0.1 μM; $CFSE^{low}$ cells). Cells were washed twice with PBS and equal numbers of cells from each population were injected i.v. (10^7 target cells).

Animals were sacrificed after 18 h and the presence of target cells in the draining lymph nodes was determined by flow cytometry.

For in vitro cytotoxicity assays, RMA target cells were loaded with the OVA-derived peptide SIINFEKL (1 μM) and labeled with a high concentration of CFSE (1 μM; $CFSE^{high}$). Nonloaded, low CFSE-labeled (0.1 μM; $CFSE^{low}$) RMA cells served as a control. Cells were washed twice with PBS and equal numbers of cells from each population were mixed. Five $\times 10^3$ cells were cocultured along with different numbers of OT-I T cells (primed) or without T cells (control) that had been primed by Pio-treated or untreated BM-DCs for 5 days.

To calculate the specific lysis of the cytotoxicity assays, the following formula was used: percent OVA-specific cytotoxicity = 100 − [100 × ($CFSE^{high}$/$CFSE^{low}$) primed/($CFSE^{high}$/$CFSE^{low}$) control].

Analysis of reactivation of memory T cells

For induction of an OVA-specific $CD8^+$ T cell memory response in vivo, $CD8^+$ T cells derived from OT-I mice carrying the congenic marker CD90.2 were transferred i.v. into C57BL/6 mice with the congenic marker CD90.1. After 24 h, the mice were immunized with OVA-expressing adenoviruses (1.10^7 PFU/mouse) i.v. After another 30 days, OVA-specific $CD8^+$ T cells were isolated by immunomagnetic separation using a $CD8^+$ T cell isolation kit (Miltenyi Biotec) followed by further purification using magnetic beads labeled with an Ab directed against CD90.2. These T cells were restimulated in vitro by either Pio-treated or untreated OVA-loaded BM-DCs as described above. After 36 h, production of IFN-γ was assessed by ELISA.

Statistical analysis

Statistical analysis was performed using Student's *t* test. Significant values are indicated as follows: *, $p < 0.05$; **, $p < 0.01$; and ***, $p < 0.001$.

Results

Activation of PPARγ leads to increased MR expression in BM-DCs

Cross-presentation of soluble OVA by murine BM-DCs is strictly dependent on the expression of the MR (8, 10), which is only expressed by a subset of these cells (8). To identify cell-intrinsic factors that may influence MR-mediated endocytosis and hence cross-presentation, we separated MR^+ BM-DCs from MR^- BM-DCs and assessed their genome-wide transcriptional profile using BeadChip Arrays. We observed that PPARγ was preferentially expressed in MR^+ BM-DCs (fold change of 2.74; $p = 0.0015$). Since activation of PPARγ has been shown to increase levels of MR-encoding mRNA (28), we investigated whether PPARγ activation results in increased MR expression in BM-DCs. Sustained activation of PPARγ by the agonist Pio during DC differentiation from bone marrow precursor cells resulted in a significant increase in the proportion of MR-expressing DCs when compared with untreated DCs (Fig. 1, *A* and *B*). To exclude that this up-regulation was due to PPARγ-independent effects of Pio, we used conditional PPARγ knockout BM-DCs that were generated by treatment of bone marrow precursor cells from $PPAR\gamma^{fl/fl}$ mice with a membrane-permeable Cre-recombinase (HTNCre). In these cells, HTNCre treatment led to a site-specific recombination resulting in deletion of exon 1 and exon 2 of the PPARγ gene in ~70–80% of all cells as described previously (23, 29). Pio-induced up-regulation of MR expression was strongly reduced in conditional PPARγ knockout DCs compared with wild-type DCs (Fig. 1, *C* and *D*), demonstrating that the effect of Pio on MR expression was indeed mediated by PPARγ.

Activation of PPARγ increases MR-mediated OVA uptake

To investigate whether the enhanced expression of the MR results in increased uptake of soluble OVA, we incubated Pio-treated and untreated wild-type BM-DCs with fluorescently labeled OVA and analyzed OVA uptake by flow-cytometry. In Pio-treated DCs, we observed a significantly increased uptake of OVA compared with untreated DCs (Fig. 2, *A* and *B*). This effect of Pio was not observed in MR-deficient DCs, demonstrating that increased OVA-uptake induced by Pio was mediated by increased expression of the MR (Fig. 2, *A* and *B*). Again, to exclude PPARγ-independent effects of Pio, we performed these experiments in conditional PPARγ knockout BM-DCs. Upon Cre-mediated PPARγ ablation, Pio did not affect the uptake of OVA in DCs (Fig. 2, *C* and *D*), confirming that enhanced MR-mediated OVA uptake by Pio was mediated by PPARγ.

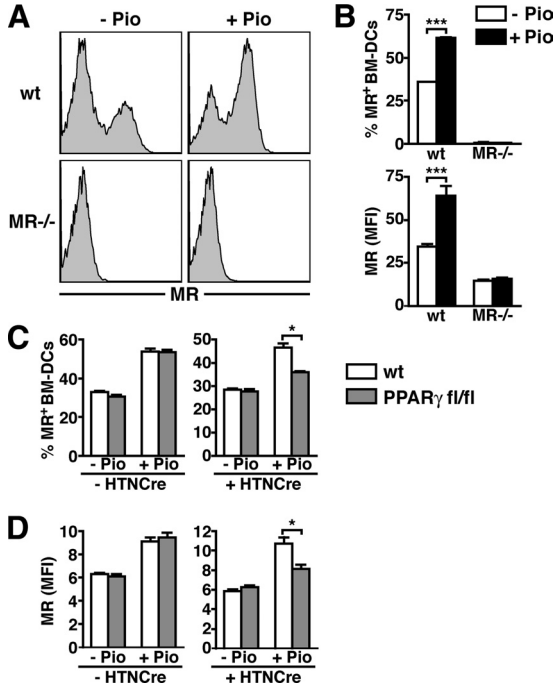

FIGURE 1. Increased MR expression after activation of PPARγ. *A*, MR expression in Pio-treated and untreated wild-type (wt) or MR-deficient BM-DCs was monitored by intracellular MR staining and analyzed by flow cytometry. *B*, Statistical analysis of cells treated as in *A*. Graphs show average percentage of MR-expressing cells (*upper panel*) and average mean fluorescence intensity (MFI) of MR expression (*lower panel*) ± SEM. *C* and *D*, Untreated (*left*) or HTNCre-treated (*right*) wild-type and $PPAR\gamma^{fl/fl}$ cells were stained for MR expression. Graphs depict average percentage of MR-expressing cells ± SEM (*C*) or average mean fluorescence intensity of MR expression ± SEM (*D*). All experiments were performed at least three times. Data of one representative experiment are shown. Within one experiment, $n \geq 3$. *, $p < 0.05$ and ***, $p < 0.001$.

Activation of PPARγ enhances cross-presentation of OVA

Since MR-internalized OVA is exclusively cross-presented on MHC I molecules (8), we investigated whether the increased MR-mediated uptake of OVA would result in increased cross-presentation. To this end, we incubated untreated and Pio-treated BM-DCs with OVA and monitored cross-presentation. BM-DCs were stained using the 25-D1.16 Ab which recognizes the OVA-derived SIINFEKL epitope when bound to the MHC I molecule Kb (30), hence detecting cross-presented OVA on APCs (8, 11, 31, 32). After incubation with OVA, cross-presentation was significantly enhanced in Pio-treated DCs when compared with untreated DCs (Fig. 3*A*). To test whether the increase in cross-presentation was relevant for activation of OVA-specific T cells, we incubated Pio-treated or untreated BM-DCs with OVA and subsequently cocultured them with the T cell hybridoma B3Z (33). Upon recognition of the OVA-derived SIINFEKL epitope complexed to the MHC I molecule Kb (i.e., cross-presented OVA), these hybridoma cells become activated and synthesize β-galactosidase under control of the IL-2 promoter. Importantly, since the activation of B3Z cells

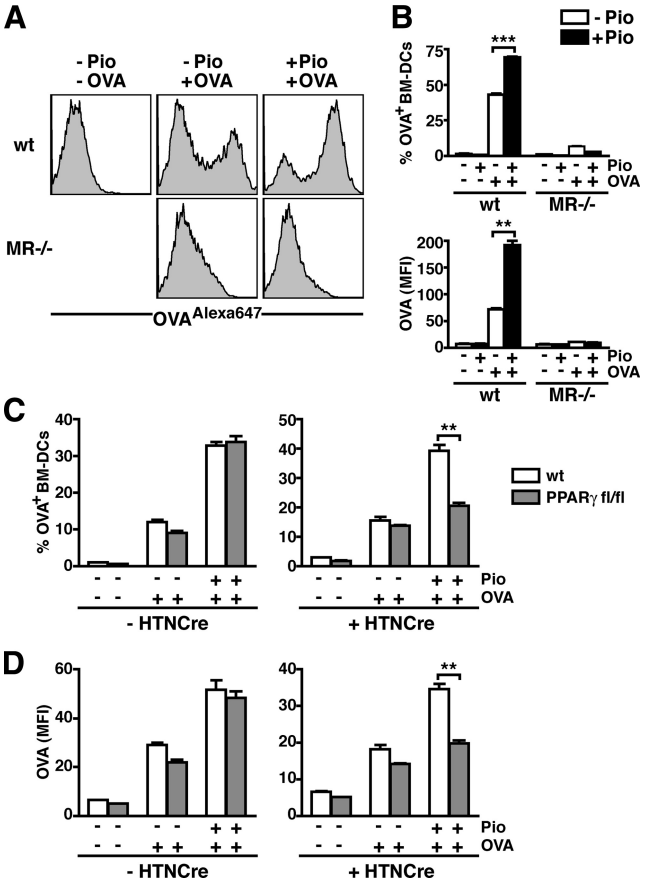

FIGURE 2. Increased MR-mediated uptake of OVA after activation of PPARγ. *A*, Pio-treated and untreated wild-type (wt) or MR-deficient DCs were incubated with fluorochrome-labeled OVA. Uptake was analyzed by flow cytometry. *B*, Statistical analysis of cells treated as in *A*. Graphs show average percentage of OVA-positive cells (*upper panel*) and average mean fluorescence intensity (MFI) of OVA uptake (*lower panel*) ± SEM. *C* and *D*, Untreated (*left*) or HTNCre-treated (*right*) wild-type and PPARγ$^{fl/fl}$ cells were incubated with fluorochrome-labeled OVA. Graphs depict percentage of OVA-positive DCs ± SEM (*C*) or average mean fluorescence intensity of OVA uptake ± SEM (*D*). All experiments were performed at least three times. Data of one representative experiment are shown. Within one experiment, $n \geq 3$. **, $p < 0.01$ and ***, $p < 0.001$.

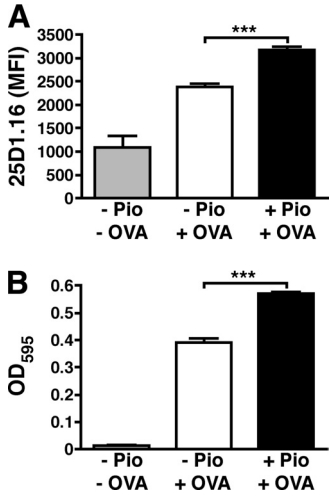

FIGURE 3. Increased cross-presentation after activation of PPARγ. *A*, Pio-treated or untreated BM-DCs were incubated with OVA. Cross-presentation of OVA was monitored by staining with the 25-D1.16 Ab and fluorescence was analyzed using the Scan^R Software. Graphs depict average mean fluorescence intensity (MFI) ± SEM. *B*, Pio-treated or untreated BM-DCs were incubated with OVA and cocultured with B3Z cells. Activation of B3Z cells was measured by spectrophotometric analysis of CPRG conversion at 595 nm. Graphs depict average OD_{595} ± SEM. All experiments were performed at least three times. Data of one representative experiment are shown. Within one experiment, $n \geq 3$. ***, $p < 0.001$.

does not depend on costimulatory signals (26, 33, 34), β-galactosidase activity directly correlates with the amount of peptide-loaded MHC I molecules on the DC surface. Activation of B3Z cells by Pio-treated BM-DCs was significantly enhanced compared with untreated DCs (Fig. 3*B*). Taken together, these data show that Pio-mediated activation of PPARγ in BM-DCs up-regulates expression of the MR, which in turn results in enhanced uptake and cross-presentation of soluble OVA.

Activation of PPARγ in BM-DCs impairs Ag-specific activation of CD8$^+$ T cells

Next, we asked whether enhanced cross-presentation by Pio-treated BM-DCs may also influence Ag-specific priming of naive OVA-specific CD8$^+$ T cells derived from TCR-transgenic OT-I mice. Apart from signal 1, namely, cross-presented OVA, these primary T cells depend on signal 2 and signal 3 for full activation (35). Priming of OT-I T cells by Pio-treated BM-DCs was clearly decreased as demonstrated by a severely diminished production of IFN-γ, which was observed for a range of DC:T cell ratios (Fig. 4*A*). Likewise, CD8$^+$ T cell proliferation, as monitored by analysis of the CFSE dilution profiles by flow cytometry, was also clearly impaired in those T cells that had been cocultured with Pio-treated BM-DCs (Fig. 4*B*). Additionally, we tested CD8$^+$ T cell effector functions, i.e., their ability to kill peptide-loaded target cells in an in vitro cytotoxicity assay. Importantly, T cells primed by Pio-treated DCs showed a markedly reduced cytotoxic activity when compared with T cells stimulated by untreated DCs (Fig. 4*C*), demonstrating that activation of PPARγ in BM-DCs indeed impaired their capacity to fully activate naive CD8$^+$ T cells despite enhanced cross-presentation.

Furthermore, we tested the ability of Pio-treated DCs to reactivate OVA-specific memory T cells that had been generated in response to an adenoviral infection in vivo. Interestingly, no influence of PPARγ on the capacity of BM-DCs to reactivate these CD8$^+$ memory T cells ex vivo was observed (Fig. 4*D*), suggesting that the effect of Pio is restricted to the modulation of primary T cell responses.

Activation of PPARγ in BM-DCs enhances expression of B7H1, thereby restricting CD8$^+$ T cell priming

To investigate whether the impaired activation of naive CD8$^+$ T cells was due to altered expression of either coinhibitory molecules or costimulatory molecules, we analyzed their expression in Pio-treated and untreated BM-DCs. Importantly, treatment of BM-DCs with Pio significantly increased the expression of B7H1 when compared with untreated cells (Fig. 5*A*). This up-regulation of B7H1 strictly correlated to the expression of the MR, as DCs internalizing large amounts of OVA via the MR showed a strongly enhanced expression of B7H1 (Fig. 5*B*). In contrast to the strong up-regulation of B7H1, expression of costimulatory molecules CD40, CD80, CD86, and ICOSL on immature BM-DCs changed only marginally after Pio treatment (supplemental Fig. 1*A*[5]). B7DC was only expressed at low levels and its expression was not altered due to the treatment with Pio (supplemental Fig. 1*B*).

[5] The online version of this article contains supplemental material.

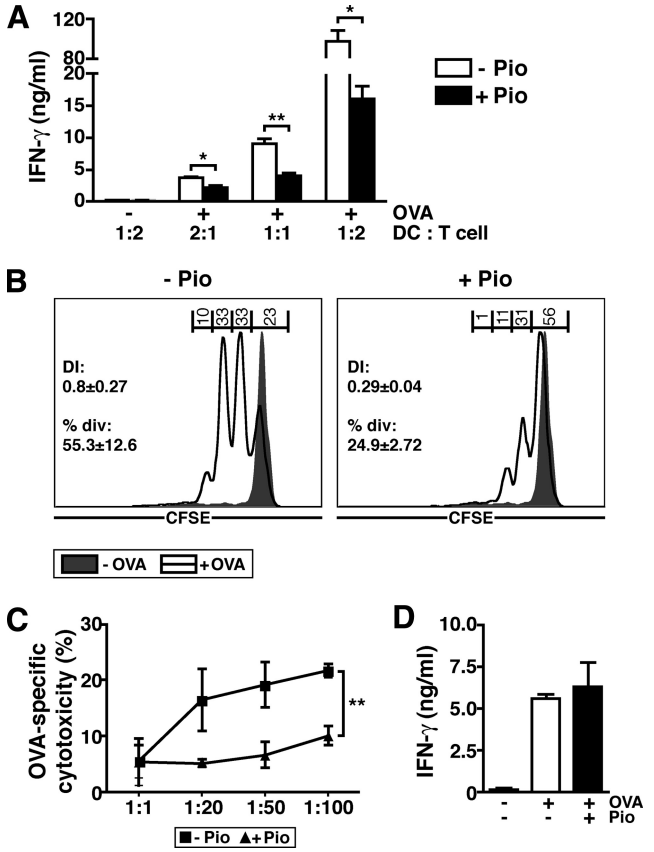

FIGURE 4. Impaired stimulation of primary T cells after activation of PPARγ. *A*, Untreated or Pio-treated BM-DCs were incubated with OVA and cocultured with naive OVA-specific $CD8^+$ T cells (OT-I) using the indicated DC:T cell ratios. T cell activation was determined by analyzing the concentration of IFN-γ in the supernatant using ELISA. Graph depicts average concentration of IFN-γ ± SEM. *B*, Untreated or Pio-treated BM-DCs were incubated with OVA and cocultured with CFSE-labeled OT-I T cells. T cell proliferation was determined by flow cytometric analysis of CFSE dilution. Numbers above the graph indicate average percentage of cells within one cycle, numbers on the left indicate the division index (DI) and percentage of divided cells (% div) ± SEM. *C*, OT-I T cells primed by Pio-treated or untreated OVA-loaded BM-DCs were incubated with peptide-loaded or unloaded fluorochrome-labeled target cells. The specific kill of peptide-loaded target cells was determined by flow cytometry. Graphs depict average proportion of specific kill ± SEM. *D*, Pio-treated or untreated BM-DCs were incubated with OVA and cocultured with OVA-specific memory T cells. Reactivation of these T cells was determined after 18 h by analyzing the concentration of IFN-γ in the supernatant using ELISA. Graph depicts average concentration of IFN-γ ± SEM. ∗, $p < 0.05$ and ∗∗, $p < 0.01$. All experiments were performed at least two times. Data of one representative experiment are shown. Within one experiment, $n \geq 3$.

To investigate whether PPARγ-mediated impairment of DC priming capacity was due to enhanced expression of B7H1, we analyzed the capacity of PPARγ-activated B7H1-deficient DCs to prime OT-I T cells. In contrast to wild-type DCs, which had an impaired capacity to activate $CD8^+$ T cells after activation of PPARγ, B7H1-deficient DCs activated OT-I T cells even more efficiently after Pio treatment as indicated by strongly enhanced production of IFN-γ (Fig. 5*C*). Furthermore, T cell proliferation was clearly increased after coincubation with Pio-treated B7H1-deficient BM-DCs compared with nontreated BM-DCs from B7H1-deficient mice (Fig. 5*D*). These results indicate that the impaired T cell activation observed in cocultures with Pio-treated wild-type BM-DCs was mediated by the up-regulation of B7H1, as

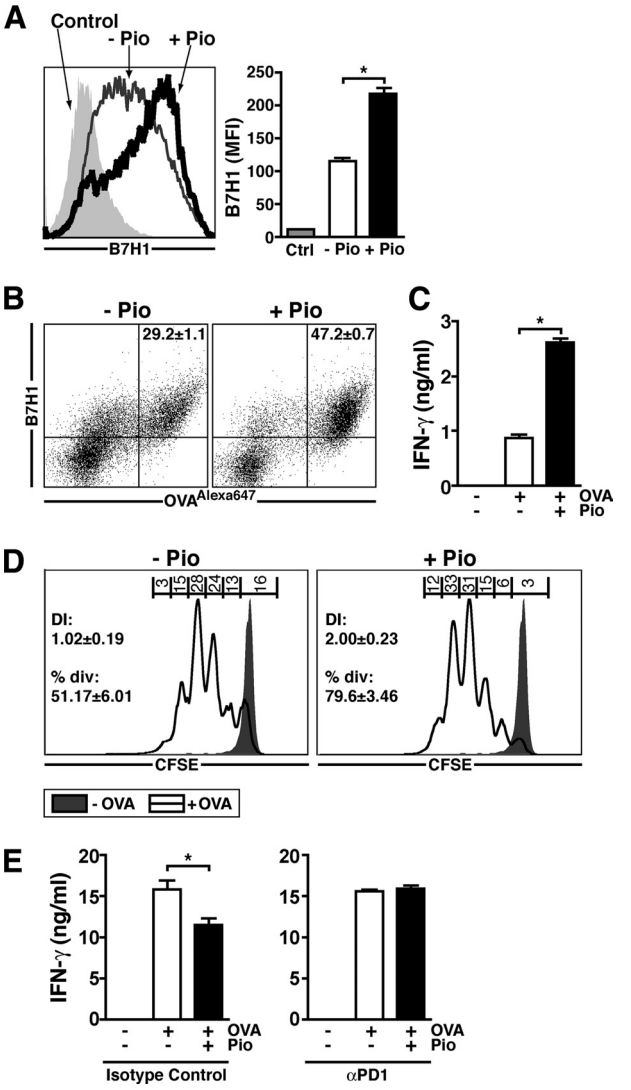

FIGURE 5. Impaired T cell stimulation after PPARγ activation is due to up-regulation of B7H1. *A*, Expression of B7H1 by Pio-treated or untreated BM-DCs was analyzed by flow cytometry. Graph shows mean fluorescence intensity of B7H1 staining and depicts average mean fluorescence intensity (MFI) ± SEM. *B*, Expression of B7H1 on Pio-treated or untreated BM-DCs after internalization of fluorochrome-labeled OVA. Numbers depict average percentage of $B7H1^+OVA^+$ BM-DCs ± SEM. *C*, Pio-treated or untreated BM-DCs from B7H1-deficient mice were incubated with OVA and cocultured with OVA-specific $CD8^+$ T cells (OT-I). T cell activation was determined by analyzing the concentration of IFN-γ in the supernatant using ELISA. Graph depicts average concentration of IFN-γ ± SEM. *D*, Untreated or Pio-treated BM-DCs from B7H1-deficient mice were incubated with OVA and cocultured with CFSE-labeled OT-I T cells. T cell proliferation was determined by flow cytometric analysis of the CFSE dilution. Numbers indicate average percentage of cells within one cycle, division index (DI), and percentage of divided cells (% div) ± SEM. *E*, Pio-treated or untreated OVA-loaded BM-DCs were cocultured with OT-I T cells in the presence of a PD1-specific blocking Ab (20 μg/ml) or the appropriate isotype control. T cell activation was determined by measuring the IFN-γ concentrations in the supernatant after 18 h using ELISA. Graphs depict average concentration of IFN-γ ± SEM. All experiments were performed at least two times. Data of one representative experiment are shown. Within one experiment, $n \geq 3$. ∗, $p < 0.05$.

in the absence of B7H1, a PPARγ-induced increase in cross-presentation results in enhanced activation of $CD8^+$ T cells by Pio-treated BM-DCs in vitro.

To further prove that reduced cross-priming after Pio treatment was due to the interaction of B7H1 expressed by DCs with PD1 on the surface of OT-I T cells (supplemental Fig. 2), we performed the cross-priming experiment in the presence of a PD1-specific blocking Ab, which prevents interaction of PD1 with B7H1 (36). Indeed, the reduced cross-priming capacity of PPARγ-activated BM-DCs was overcome in the presence of the blocking Ab, demonstrating that the effect of PPARγ on T cell priming depended on the interaction of B7H1 on BM-DCs with PD1 on T cells (Fig. 5*E*).

PPARγ activation in vivo results in impaired CD8$^+$ T cell priming by up-regulation of B7H1

Finally, we investigated whether the effect of PPARγ activation on cross-presentation and on T cell activation can also be observed in vivo. To this end, mice were treated for 7 days with Pio or the vehicle only by daily oral gavage before they were injected with fluorochrome-labeled OVA. After 45 min, splenic DCs were isolated and analyzed for uptake of OVA and expression of the MR. Confirming our results obtained from Pio-treated BM-DCs, splenic DCs from Pio-treated mice also showed an increase in the proportion of MR-expressing DCs, which in turn resulted in an increased uptake of OVA in vivo (Fig. 6*A*).

To determine whether the increased uptake of OVA in vivo also resulted in enhanced cross-presentation of OVA-derived peptides, splenic DCs from OVA-injected Pio-treated or vehicle-treated mice were isolated and incubated with the costimulatory-independent B3Z T cell hybridoma ex vivo. Splenic DCs from Pio-treated mice showed a clearly enhanced activation of B3Z cells (Fig. 6*B*), demonstrating that cross-presentation in Pio-treated mice was indeed enhanced.

Next, we cocultured OVA-pulsed splenic DCs from Pio-treated or vehicle-treated mice ex vivo with naive CD8$^+$ T cells from OT-I mice. CD8$^+$ T cell activation by Pio-treated splenic DCs was impaired when compared with untreated DCs as demonstrated by a decreased production of IL-2 and IFN-γ (Fig. 6*C*). This difference in T cell activation was also observed after restimulation of equal numbers of OVA-specific CD8$^+$ T cells with anti-CD3 after 5 days of priming by Pio-treated splenic DCs (Fig. 6*C*), which suggests that naive T cells primed by Pio-treated DCs did not undergo proper functional differentiation and exhibit impaired effector functions upon reactivation.

Additionally, we analyzed the cytotoxic activity of activated Ag-specific T cells in vivo (27). To this end, we immunized Pio-treated or vehicle-treated wild-type mice with either Pio-treated or untreated BM-DCs loaded with OVA. After 5 days, these mice were injected with nonloaded and peptide-loaded fluorochrome-labeled target cells and the specific elimination of the peptide-loaded target cells in vivo was monitored by flow cytometry. Importantly, no cytotoxic activity of OVA-specific T cells was detectable in Pio-treated mice in contrast to vehicle-treated animals (Fig. 6*D*), demonstrating that activation of PPARγ clearly diminished CD8$^+$ T cell priming in vivo.

To analyze whether the impaired T cell activation by Pio-treated splenic DCs was also mediated by B7H1, we cocultured OVA-loaded splenic DCs from Pio-treated or untreated B7H1-deficient mice with OT-I T cells. Importantly, T cell activation was no longer impaired when T cells were cocultured with splenic DCs isolated from Pio-treated B7H1-deficient mice (Fig. 6*E*), indicating that the impairment of cross-priming by splenic DCs after PPARγ activation in vivo was also mediated by up-regulation of B7H1.

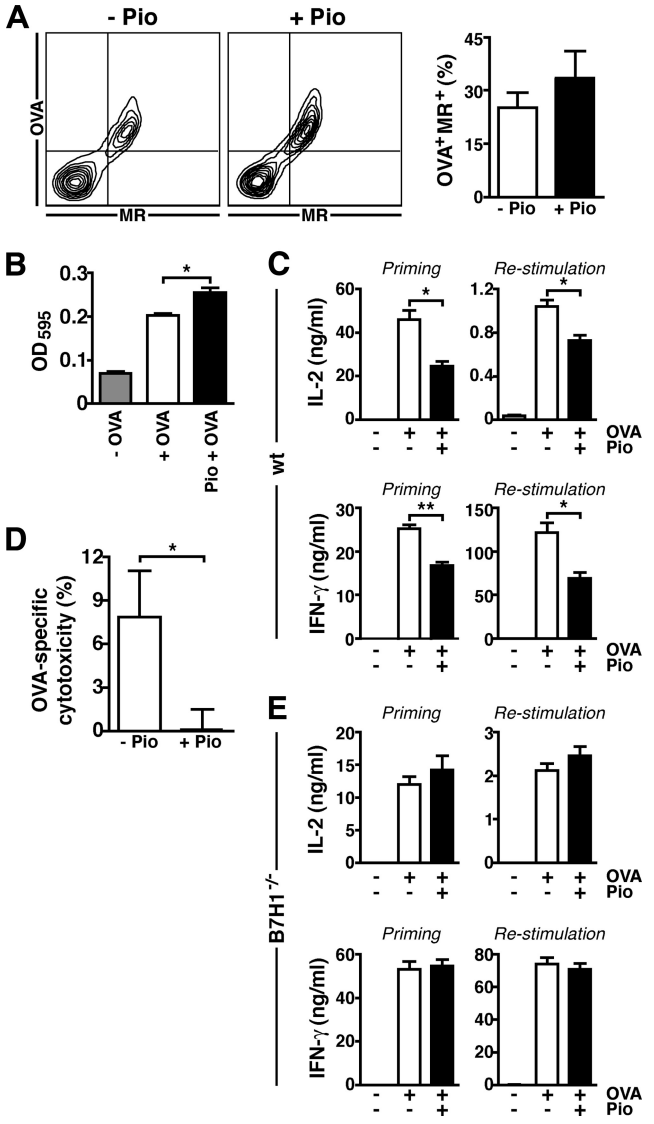

FIGURE 6. Also in splenic DCs, activation of PPARγ increased cross-presentation but impaired T cell activation due to up-regulation of B7H1. *A*, Pio- or vehicle-treated mice were injected with fluorochrome-labeled OVA. CD11c$^+$ splenic DCs were isolated by magnetic purification; OVA uptake and MR expression were determined by flow cytometry. Graphs depict average percentage of MR$^+$OVA$^+$ splenic DCs ± SEM. *B*, CD11c$^+$ splenic DCs from Pio-treated or untreated OVA-challenged mice were isolated by magnetic purification, and cocultured with B3Z cells. Activation of B3Z cells was determined by spectrophotometric analysis of CPRG conversion at 595 nm. Graph depicts average OD_{595} ± SEM. *C*, Splenic DCs from Pio- or vehicle-treated wild-type mice were isolated by magnetic purification, and cocultured with OT-I T cells. T cell activation was determined by secretion of IL-2 and IFN-γ (priming). After 5 days of cocultivation, T cells were restimulated with an anti-CD3 Ab and IL-2 and IFN-γ secretion was determined by ELISA (restimulation). Graphs depict average concentration of IL-2 and IFN-γ ± SEM. *D*, Pio-treated or vehicle-treated mice were immunized with Pio-treated or untreated OVA-loaded BM-DCs. After 5 days, peptide-loaded or nonloaded fluorochrome-labeled target cells were transferred into these mice. The specific elimination of peptide-loaded target cells was monitored by flow cytometry. Graphs depict average percentage of specific kill ± SEM. *E*, Splenic DCs from Pio- or vehicle-treated B7H1-deficient mice were isolated by magnetic purification, incubated with OVA, and cocultured with OT-I T cells. T cell activation before (priming) and after restimulation was determined by secretion of IL-2 and IFN-γ. Graphs depict average concentration of IL-2 and IFN-γ ± SEM. All experiments were performed at least two times. Data of one representative experiment are shown. Within one experiment, $n \geq 3$. *, $p < 0.05$ and **, $p < 0.01$.

Discussion

In this study, we investigated the effect of PPARγ activation in DCs on cross-presentation of soluble OVA and on cross-priming of OVA-specific $CD8^+$ T cells. We demonstrated that Pio treatment both in vitro and in vivo increased MR-mediated uptake and cross-presentation of OVA. Concurrently, PPARγ strongly enhanced the expression of the coinhibitory molecule B7H1 in DCs. Increased cross-presentation combined with enhanced coinhibitory signaling resulted in impaired activation of naive OVA-specific $CD8^+$ T cells.

In BM-DCs, MR-bearing DCs have been shown to be responsible for cross-presentation of OVA (8). Activation of PPARγ by its agonist Pio increased the proportion of MR-bearing DCs and, in consequence, increased cross-presentation of OVA. In conditional PPARγ knockout BM-DCs, Pio-mediated up-regulation of MR expression and OVA uptake was nearly abolished, demonstrating that the effects of Pio treatment were indeed mediated by PPARγ. The conditional PPARγ knockout was achieved by treatment of bone marrow precursor cells with a membrane-permeable Cre recombinase, an approach that has been demonstrated to impede ~70–80% of PPARγ expression (23). Since the reduction of MR expression in the conditional PPARγ knockout cells was 66.7% of the total Pio effect (Fig. 1*D*) and the reduction of OVA uptake in these cells was 79.2% of the total Pio effect (Fig. 2*D*), the residual activation is likely to be due to the incomplete ablation of PPARγ activity. In untreated PPARγ knockout DCs, MR expression remained unaltered (Fig. 1*C*), indicating that the baseline expression of the MR is PPARγ independent and activation of PPARγ leads to an additional increase in MR-bearing DCs.

For splenic DCs, it has been shown extensively that cross-presentation occurs preferentially in a subset of DCs, namely, in those bearing the surrogate marker CD8α (37). In a previous study, we demonstrated that a subpopulation of CD8α-bearing DCs expresses the MR, which directs OVA specifically toward cross-presentation, whereas MR expression was absent in CD8α-negative DCs (8). In this study, we demonstrated that PPARγ activation increased MR expression, but it did not alter the proportion of CD8α DCs (data not shown), indicating that the proportion of MR-bearing DCs within the $CD8\alpha^+$ DCs had increased.

The observed increase in MR expression resulted in increased uptake and cross-presentation of OVA both by BM-DCs and by splenic DCs. Cross-priming of $CD8^+$ T cells, however, not only depends on strong cross-presentation, but requires additional signaling via costimulatory molecules and proinflammatory cytokines and can be impeded by the expression of coinhibitory molecules. Impaired DC signaling via costimulatory molecules and proinflammatory cytokines mediated by PPARγ has already been demonstrated (22, 23). We now demonstrate that in immature DCs, activation of PPARγ leads to up-regulation of B7H1. Importantly, PPARγ-mediated up-regulation of B7H1 seemed to be the dominant signal for PPARγ-mediated impairment of $CD8^+$ T cell activation by DCs; as in the absence of B7H1, $CD8^+$ T cell activation was restored. The combined action of PPARγ on DCs by increasing cross-presentation and by simultaneously enhancing B7H1 expression enables a very potent inhibitory interaction of DCs with Ag-specific $CD8^+$ T cells and depicts a novel mechanism of $CD8^+$ T cell inactivation. Up-regulation of B7H1 might also explain the strongly reduced effector function of $CD8^+$ T cells primed by PPARγ-activated DCs in vitro and in vivo, as demonstrated by their reduced cytotoxicity both in the murine system (Fig. 6*D*) and in the human system as previously described (22). In vivo, this mechanism of tolerance induction might be used by endogenous PPARγ ligands under physiological conditions. One factor that might induce such effects could be IL-4, a Th2 cytokine with anti-inflammatory properties (38–40). IL-4 has been shown to induce expression of both PPARγ and its endogenous ligands in macrophages (41). Following this line, the PPARγ-mediated induction of $CD8^+$ T cell tolerance described in this study might help to explain some of the anti-inflammatory effects induced by IL-4.

Remarkably, the inhibitory effect of Pio on $CD8^+$ T cell activation seems to be restricted to the activation of primary CTLs, as Pio-treated DCs did not exhibit an impaired capacity to reactivate OVA-specific memory T cells in vitro when compared with untreated DCs. These findings extend previous observations of other groups demonstrating that activation of memory T cells by professional APCs primarily depends on Ag presentation (signal 1) and has been shown to be largely independent of the expression of costimulatory molecules (signal 2) in vitro (42, 43). Our data now suggest, that the activation of memory T cells by professional APCs might also be independent of inhibitory signaling mediated by up-regulation of B7H1.

Taken together, our data provide a new molecular mechanism for PPARγ-induced $CD8^+$ T cell tolerance, which is mediated by the combined action of increased cross-presentation and enhanced signaling via the coinhibitory molecule B7H1. This mechanism provides new insights into the molecular mechanisms of T cell inactivation and might thus open new opportunities for therapeutic intervention in $CD8^+$ T cell-mediated autoimmune diseases.

Acknowledgments

We thank Indra Dani and Andreas Kautz for excellent technical assistance, Dirk Stabenow for support using the Scan^R system, M. Nussenzweig for $MR^{-/-}$ mice, W. Heath for OT-I mice, L. Chen for $B7H1^{-/-}$ mice, and R. Germain and J. Yewdell for 25-D1.16 Ab. We acknowledge the technical support of the Flow Cytometry Core Facility at the Institutes of Molecular Medicine and Experimental Immunology as well as of the central animal facilities of the medical faculty of the University of Bonn (House for Experimental Therapy).

Disclosures

The authors have no financial conflict of interest.

References

1. Mellman, I., and R. M. Steinman. 2001. Dendritic cells: specialized and regulated antigen processing machines. *Cell* 106: 255–258.
2. Trombetta, E. S., M. Ebersold, W. Garrett, M. Pypaert, and I. Mellman. 2003. Activation of lysosomal function during dendritic cell maturation. *Science* 299: 1400–1403.
3. Bevan, M. J. 1976. Cross-priming for a secondary cytotoxic response to minor H antigens with H-2 congenic cells which do not cross-react in the cytotoxic assay. *J. Exp. Med.* 143: 1283–1288.
4. Kurts, C., W. R. Heath, F. R. Carbone, J. Allison, J. F. Miller, and H. Kosaka. 1996. Constitutive class I-restricted exogenous presentation of self antigens in vivo. *J. Exp. Med.* 184: 923–930.
5. Albert, M. L., B. Sauter, and N. Bhardwaj. 1998. Dendritic cells acquire antigen from apoptotic cells and induce class I-restricted CTLs. *Nature* 392: 86–89.
6. Morgan, D. J., H. T. Kreuwel, and L. A. Sherman. 1999. Antigen concentration and precursor frequency determine the rate of $CD8^+$ T cell tolerance to peripherally expressed antigens. *J. Immunol.* 163: 723–727.
7. Huang, A. Y., P. Golumbek, M. Ahmadzadeh, E. Jaffee, D. Pardoll, and H. Levitsky. 1994. Role of bone marrow-derived cells in presenting MHC class I-restricted tumor antigens. *Science* 264: 961–965.
8. Burgdorf, S., A. Kautz, V. Bohnert, P. A. Knolle, and C. Kurts. 2007. Distinct pathways of antigen uptake and intracellular routing in CD4 and CD8 T cell activation. *Science* 316: 612–616.
9. Burgdorf, S., and C. Kurts. 2008. Endocytosis mechanisms and the cell biology of antigen presentation. *Curr. Opin. Immunol.* 20: 89–95.
10. Burgdorf, S., V. Lukacs-Kornek, and C. Kurts. 2006. The mannose receptor mediates uptake of soluble but not of cell-associated antigen for cross-presentation. *J. Immunol.* 176: 6770–6776.
11. Burgdorf, S., C. Scholz, A. Kautz, R. Tampe, and C. Kurts. 2008. Spatial and mechanistic separation of cross-presentation and endogenous antigen presentation. *Nat. Immunol.* 9: 558–566.
12. Janeway, C. A., Jr., and R. Medzhitov. 2002. Innate immune recognition. *Annu. Rev. Immunol.* 20: 197–216.

13. Chen, L. 2004. Co-inhibitory molecules of the B7-CD28 family in the control of T-cell immunity. *Nat. Rev.* 4: 336–347.
14. Bardot, O., T. C. Aldridge, N. Latruffe, and S. Green. 1993. PPAR-RXR heterodimer activates a peroxisome proliferator response element upstream of the bifunctional enzyme gene. *Biochem. Biophys. Res. Commun.* 192: 37–45.
15. Jiang, C., A. T. Ting, and B. Seed. 1998. PPAR-γ agonists inhibit production of monocyte inflammatory cytokines. *Nature* 391: 82–86.
16. Ricote, M., A. C. Li, T. M. Willson, C. J. Kelly, and C. K. Glass. 1998. The peroxisome proliferator-activated receptor-γ is a negative regulator of macrophage activation. *Nature* 391: 79–82.
17. Yang, X. Y., L. H. Wang, T. Chen, D. R. Hodge, J. H. Resau, L. DaSilva, and W. L. Farrar. 2000. Activation of human T lymphocytes is inhibited by peroxisome proliferator-activated receptor γ (PPARγ) agonists: PPARγ co-association with transcription factor NFAT. *J. Biol. Chem.* 275: 4541–4544.
18. Von Knethen, A., and B. Brune. 2002. Activation of peroxisome proliferator-activated receptor γ by nitric oxide in monocytes/macrophages down-regulates $p47^{phox}$ and attenuates the respiratory burst. *J. Immunol.* 169: 2619–2626.
19. Cunard, R., Y. Eto, J. T. Muljadi, C. K. Glass, C. J. Kelly, and M. Ricote. 2004. Repression of IFN-γ expression by peroxisome proliferator-activated receptor γ. *J. Immunol.* 172: 7530–7536.
20. Sakamoto, J., H. Kimura, S. Moriyama, H. Odaka, Y. Momose, Y. Sugiyama, and H. Sawada. 2000. Activation of human peroxisome proliferator-activated receptor (PPAR) subtypes by pioglitazone. *Biochem. Biophys. Res. Commun.* 278: 704–711.
21. Racke, M. K., A. R. Gocke, M. Muir, A. Diab, P. D. Drew, and A. E. Lovett-Racke. 2006. Nuclear receptors and autoimmune disease: the potential of PPAR agonists to treat multiple sclerosis. *J. Nutr.* 136: 700–703.
22. Nencioni, A., F. Grunebach, A. Zobywlaski, C. Denzlinger, W. Brugger, and P. Brossart. 2002. Dendritic cell immunogenicity is regulated by peroxisome proliferator-activated receptor γ. *J. Immunol.* 169: 1228–1235.
23. Klotz, L., I. Dani, F. Edenhofer, L. Nolden, B. Evert, B. Paul, W. Kolanus, T. Klockgether, P. Knolle, and L. Diehl. 2007. Peroxisome proliferator-activated receptor γ control of dendritic cell function contributes to development of $CD4^+$ T cell anergy. *J. Immunol.* 178: 2122–2131.
24. Lutz, M. B., N. Kukutsch, A. L. Ogilvie, S. Rossner, F. Koch, N. Romani, and G. Schuler. 1999. An advanced culture method for generating large quantities of highly pure dendritic cells from mouse bone marrow. *J. Immunol. Methods* 223: 77–92.
25. Chemnitz, J. M., J. Driesen, S. Classen, J. L. Riley, S. Debey, M. Beyer, A. Popov, T. Zander, and J. L. Schultze. 2006. Prostaglandin E2 impairs $CD4^+$ T cell activation by inhibition of lck: implications in Hodgkin's lymphoma. *Cancer Res.* 66: 1114–1122.
26. Karttunen, J., S. Sanderson, and N. Shastri. 1992. Detection of rare antigen-presenting cells by the *lacZ* T-cell activation assay suggests an expression cloning strategy for T-cell antigens. *Proc. Natl. Acad. Sci. USA* 89: 6020–6024.
27. Berg, M., G. Wingender, D. Djandji, S. Hegenbarth, F. Momburg, G. Hammerling, A. Limmer, and P. Knolle. 2006. Cross-presentation of antigens from apoptotic tumor cells by liver sinusoidal endothelial cells leads to tumor-specific $CD8^+$ T cell tolerance. *Eur. J. Immunol.* 36: 2960–2970.
28. Coste, A., M. Dubourdeau, M. D. Linas, S. Cassaing, J. C. Lepert, P. Balard, S. Chalmeton, J. Bernad, C. Orfila, J. P. Seguela, and B. Pipy. 2003. PPARγ promotes mannose receptor gene expression in murine macrophages and contributes to the induction of this receptor by IL-13. *Immunity* 19: 329–339.
29. He, W., Y. Barak, A. Hevener, P. Olson, D. Liao, J. Le, M. Nelson, E. Ong, J. M. Olefsky, and R. M. Evans. 2003. Adipose-specific peroxisome proliferator-activated receptor γ knockout causes insulin resistance in fat and liver but not in muscle. *Proc. Natl. Acad. Sci. USA* 100: 15712–15717.
30. Porgador, A., J. W. Yewdell, Y. Deng, J. R. Bennink, and R. N. Germain. 1997. Localization, quantitation, and in situ detection of specific peptide-MHC class I complexes using a monoclonal antibody. *Immunity* 6: 715–726.
31. Houde, M., S. Bertholet, E. Gagnon, S. Brunet, G. Goyette, A. Laplante, M. F. Princiotta, P. Thibault, D. Sacks, and M. Desjardins. 2003. Phagosomes are competent organelles for antigen cross-presentation. *Nature* 425: 402–406.
32. Castellino, F., P. E. Boucher, K. Eichelberg, M. Mayhew, J. E. Rothman, A. N. Houghton, and R. N. Germain. 2000. Receptor-mediated uptake of antigen/heat shock protein complexes results in major histocompatibility complex class I antigen presentation via two distinct processing pathways. *J. Exp. Med.* 191: 1957–1964.
33. Sanderson, S., and N. Shastri. 1994. LacZ inducible, antigen/MHC-specific T cell hybrids. *Int. Immunol.* 6: 369–376.
34. Zeelenberg, I. S., M. Ostrowski, S. Krumeich, A. Bobrie, C. Jancic, A. Boissonnas, A. Delcayre, J. B. Le Pecq, B. Combadiere, S. Amigorena, and C. Thery. 2008. Targeting tumor antigens to secreted membrane vesicles in vivo induces efficient antitumor immune responses. *Cancer Res.* 68: 1228–1235.
35. Hogquist, K. A., S. C. Jameson, W. R. Heath, J. L. Howard, M. J. Bevan, and F. R. Carbone. 1994. T cell receptor antagonist peptides induce positive selection. *Cell* 76: 17–27.
36. Ansari, M. J., A. D. Salama, T. Chitnis, R. N. Smith, H. Yagita, H. Akiba, T. Yamazaki, M. Azuma, H. Iwai, S. J. Khoury, H. Auchincloss, Jr., and M. H. Sayegh. 2003. The programmed death-1 (PD-1) pathway regulates autoimmune diabetes in nonobese diabetic (NOD) mice. *J. Exp. Med.* 198: 63–69.
37. den Haan, J. M., S. M. Lehar, and M. J. Bevan. 2000. $CD8^+$ but not $CD8^-$ dendritic cells cross-prime cytotoxic T cells in vivo. *J. Exp. Med.* 192: 1685–1696.
38. Ohmori, Y., and T. A. Hamilton. 1998. STAT6 is required for the anti-inflammatory activity of interleukin-4 in mouse peritoneal macrophages. *J. Biol. Chem.* 273: 29202–29209.
39. Wei, R., and G. M. Jonakait. 1999. Neurotrophins and the anti-inflammatory agents interleukin-4 (IL-4), IL-10, IL-11 and transforming growth factor-β1 (TGF-β1) down-regulate T cell costimulatory molecules B7 and CD40 on cultured rat microglia. *J. Neuroimmunol.* 95: 8–18.
40. Zhao, W., W. Xie, Q. Xiao, D. R. Beers, and S. H. Appel. 2006. Protective effects of an anti-inflammatory cytokine, interleukin-4, on motoneuron toxicity induced by activated microglia. *J. Neurochem.* 99: 1176–1187.
41. Lin, S. X., W. G. Mallet, A. Y. Huang, and F. R. Maxfield. 2004. Endocytosed cation-independent mannose 6-phosphate receptor traffics via the endocytic recycling compartment en route to the *trans*-Golgi network and a subpopulation of late endosomes. *Mol. Biol. Cell* 15: 721–733.
42. Mullbacher, A., and K. Flynn. 1996. Aspects of cytotoxic T cell memory. *Immunol. Rev.* 150: 113–127.
43. Flynn, K., and A. Müllbacher. 1996. Memory alloreactive cytotoxic T cells do not require costimulation for activation in vitro. *Immunol. Cell Biol.* 74: 413–420.